

MICROSTRUCTURAL AND PHASE STUDY OF Y_2O_3 DOPED HYDROXYAPATITE/ Al_2O_3 BIOCOSCOMPOSITES

K. E. ÖKSÜZ^{a*}, A. ÖZER^a

Department of Metallurgical & Materials Engineering, Cumhuriyet University, 58140, Sivas, Turkey

Hydroxyapatite is the mineral component of natural hard tissues and, as such, it has been studied extensively as a candidate biomaterial for its use in prosthetic applications. This study presents the fabrication and characterization of Y_2O_3 doped HA- Al_2O_3 composite materials. Hydroxyapatite (HA) powder was obtained from bovine bones (BHA) via calcination technique. Fine powders of HA/ Al_2O_3 were admixed with 0.5 and 1 wt % Y_2O_3 powders. Powder-compacts were sintered at 1550°C for 4h. SEM, EDS and X-ray diffraction studies were conducted. The effect of increasing Y_2O_3 content on surface morphology, elemental distribution and phase evaluation was investigated in hydroxyapatite/ Al_2O_3 biocomposite materials.

(Received December 14, 2015; Accepted February 15, 2016)

Keywords: Aluminum oxide, Hydroxyapatite, Phase evaluation, X-ray diffraction, Yttria.

1. Introduction

Hydroxyapatite (HA, $Ca_{10}(PO_4)_6(OH)_2$) materials are very popular for bone restorations since they accelerate the bone growth around the implant due to their chemical and crystallographic similarity to the human carbonated apatite [1]. HA can be synthesized/derived from natural sources [2]. Because bone defects arisen from cancer, injury and accident are the most common case in the clinic, a mass amount of HA is needed for restoration of bone defects [3]. Nevertheless, the mechanical properties of HA are poor, especially in wet environment. Therefore, ceramics of pure HA cannot be suggested for use in heavy-loaded implants, such as artificial bones or teeth. They can only be used at non-loading applications, such as graft materials. To improve the mechanical reliability of HA ceramics, i.e. to increase their fracture toughness, incorporation of metallic materials, ceramic oxides [4-8], whiskers, or fibers, have been suggested. However, the whiskers are not recommended in biomedical applications because of their potential carcinogenicity [9]. The HA derived from the bovine bone is advantageous. It is environment friendly and effective when the HA is directly obtained from bones which are regarded as food junk. In this experimental study, we present the production and the characterization of HA- Al_2O_3 and Y_2O_3 doped HA- Al_2O_3 composites, produced via sintering of powder compacts. Y_2O_3 was doped as 0.5 and 1 wt % into composite. The microstructural observations, elemental distribution, phase evaluation and crystallographic analysis were carried out for the produced samples.

2. Materials and experimental procedure

Bovine femoral bones were cut into small pieces and deproteinized in an alkali solution of 1 wt% sodium hypochlorite. After washing and drying, the bone pieces were calcined at 850°C for 4 h in air to totally eliminate any risk of transmitting diseases. The calcined bone pieces were crushed and then ball-milled until fine powders (i.e., with particles of submicron average size, d_{mean}) of apatite (BHA) was obtained [10,16]. BHA-powders were mixed with 50 wt % Al_2O_3

* Corresponding author: kerimemreoksuz@gmail.com

powder with a mean particle size of 1 micron. The HA-Al₂O₃ powder mixture was well homogenized with 0.5 and 1.0 wt % Y₂O₃ by wet ball-milling and donated as BHAA, 0.5BHAA, 1BHAA respectively. The suspensions were dried and the obtained powders were uniaxially pressed at 350MPa to form cylindrical pellets with a diameter of 13 mm and height of 10 mm, according to the British Standard for compression tests. Fig. 1a, 1a', 1b and 1c represents the head of the femur (the inset picture is the bovine femoral head), SEM image of bovine bone calcined at 850°C 2h. and ground initial powders after ball milling for 6 days, respectively. The green bodies were sintered at 1550°C for 4 h in air. The sintered samples were analysed by scanning electron microscopy (SEM), energy-dispersive spectroscopy (EDS) and X-ray diffraction (XRD) for further investigation of grain morphology, shape, size and phase formation.

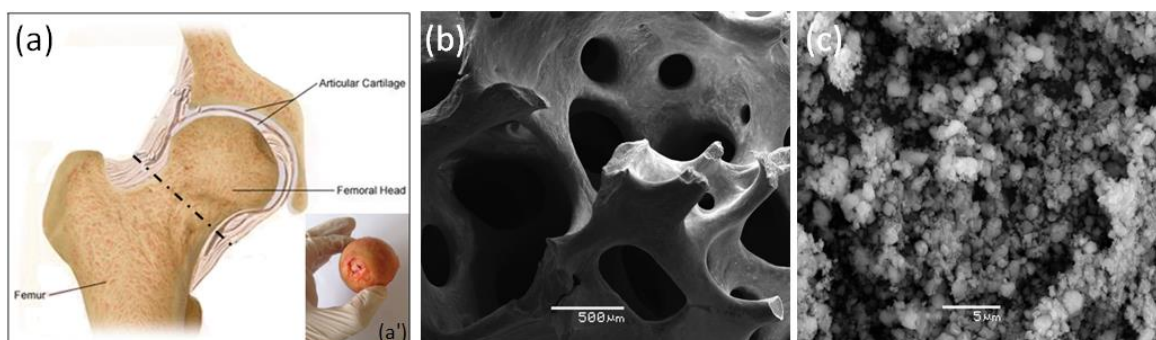


Fig. 1. (a) Schematic view of the femoral head, (a') The head of the femur. The inset picture of the femoral head after removal, (b) SEM images of bovine bone calcined at 850°C 2h. and (c) ground wet powders after ball milling for 6 days.

3. Results and discussion

The results of the crystallographic analysis of the produced samples, carried out with X-ray diffraction, are summarized in Fig. 2. In all cases, the diffractograms have predominantly registered the Hibonite phase – (CaO (Al₂O₃)₆), matched for every sample (ICSD card no. 76-0665) due to the dissolution of CaO from HA and reacts with Al₂O₃ which occurs 50wt% in the composite. X-ray diffraction patterns of HA/Al₂O₃ composite powders show that the peaks correspond to HA and Al₂O₃ phases, confirming that Al₂O₃ is effectively incorporated into the HA matrix by forming hibonite and other registered main phases were HA, calcium yttrium phosphate, AlYO₃. Ca-Y-P related phases are composed by increasing Y content and after 0.5wt% of Y₂O₃ addition, the phases were immiscible in Ca-P as understood from the formation of Al-Y related phases. CaP phase peaks increase due to the dissolution of Al₂O₃ from CaO to form CaP with Y₂O₃. Y atoms share the Ca sites to form Ca-Y-P related phase by decreasing the Ca amount in component from 10 to 9 which is attributed to the Y doping into Ca-P phase. The symmetry of the HA structure is deteriorated due to the Y incorporation into Ca sites, the lattice is distorted by increasing the 2θ about 0.2° and changes the peak heights at 53.1° and 53.6°, especially. As very well-known from crystallographic theory, the more the element in a lattice, the more the visible peaks but in lower intensity.

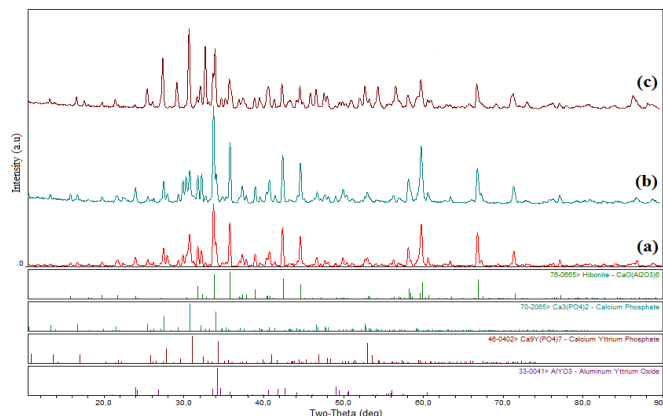
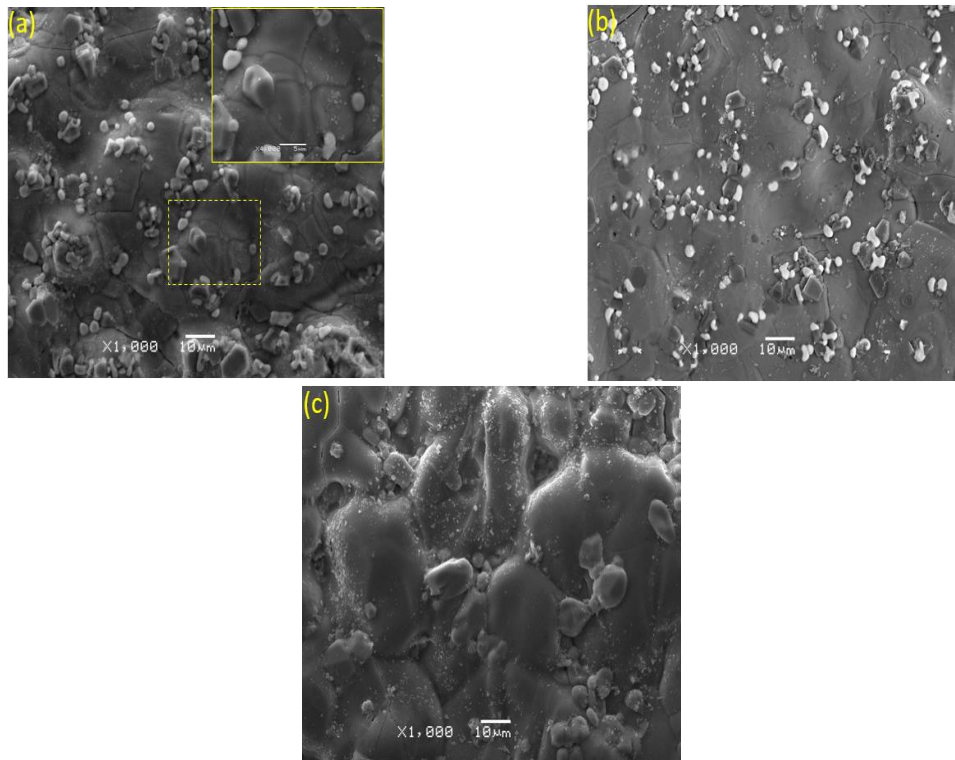


Fig. 2. XRD patterns of biocomposite samples obtained with various amounts of Y_2O_3 after sintering at temperature of $1550^\circ C$ 4h. (a) BHAA, (b) 0.5BHAA, (c) 1BHAA.

Fig. 3 (a-c) shows the representative SEM images of the sintering products of biocomposites, obtained by sintering at $1550^\circ C$ for 4h. Fig. 3 reveals that the homogeneous morphology were obtained for all compositions after sintering. The SEM images were obtained from secondary electron investigation mode to evaluate the grain morphologies along with the formed phases among the grain boundaries. Energy dispersive X-ray spectroscopy (SEM/EDS) were involved to explore the morphology structures and elemental composition of the biocomposite samples after sintering. As seen from Fig. 3. (a-c), the hexagonal shaped grown structures were found to be as Ca-Al-O phases as illustrated in EDS. A dense and fine grained microstructure was obvious and single crystal from gas phase evaporation-precipitation mechanism is seen as hexagonal shapes among the grain boundaries to decrease the grain boundary energy and led to densification by liquid phase formation as very well understood from the fast grown grains of Ca-P-O phase labeled as HA in XRD. In Fig. 3a, the grain morphology is homogeneous and dense with CaO- Al_2O_3 structures grown from the gas phase reaction as single crystals, and agglomeration of grown phases are not in progress. In Fig. 3b, increasing Y content drives the liquid phase formation and agglomeration of grown hexagonal shapes are in progress due to the grain growth and smoother surface morphology. Besides, Y content may also favor the formation of a new phase with Ca deficiency labeled as $(Ca_9Y)(PO_4)_7$ phase in XRD and a new eutectic structure $AlYO_3$ which may correspond from the grain growth. Very fine dust-like powders on grains as seen in Fig. 3b, are believed to be the initial formation and growth powders of the accompanying phases other than Ca-P-O main phase. The surface diffusion and solution-reprecipitation mechanism may be the main transport phenomena for the dust like distribution of mentioned phases. Moreover, Fig. 3c illustrates the grain growth of main phase with the agglomerated hexagonal shaped single crystal grown structures. Also, the dust like powders are in progress even in a growing manner, and the grain sizes are significantly different from each other as to be 6.5 ± 0.3 , 15.1 ± 0.6 , and 26.4 ± 0.8 microns for Fig. 3 (a-c), respectively.



*Fig. 3. SEM images of the biocomposites sintered at 1550°C for 4h.
(a) BHAA, (b) 0.5BHAA, (c) 1BHAA.*

Typical EDS spectra representing various elements found in the sintering products are shown in Fig. 4 (a-f). Fig. 4 (b-d-f) represents the distribution of chemical elements on the sintered surfaces. These images demonstrate good homogeneity of the surfaces. The distribution of chemical elements in both cases is almost uniform. The energy peaks corresponding to Ca, P and Al elements from EDS analysis are very strong for all compositions (Fig. 4. (b)-(d)-(f)) while the yttrium element can be detected for 0.5BHAA and 1BHAA biocomposites only in Fig. 4 (d)-(f) by increasing Y addition. Results in Fig. 4. also indicate that the precipitates formed on the surface of the composite is calcium hibonite containing calcium, aluminum rich phase, which coincides with the XRD results. By increasing Y content, the hibonite phase is tend to be dissolved in Ca-P phase due to liquid phase formation and grain growth characteristics of the products. As illustrated in XRD, the hibonite phase decreases against Ca-P by increasing Y content which corresponds from the eutectic phase formation. The grain growth is attributed to the Y_2O_3 addition to form eutectic with Al_2O_3 as transient liquid phase. As known, Y_2O_3 is the polymorph of Al_2O_3 to form solid solution.

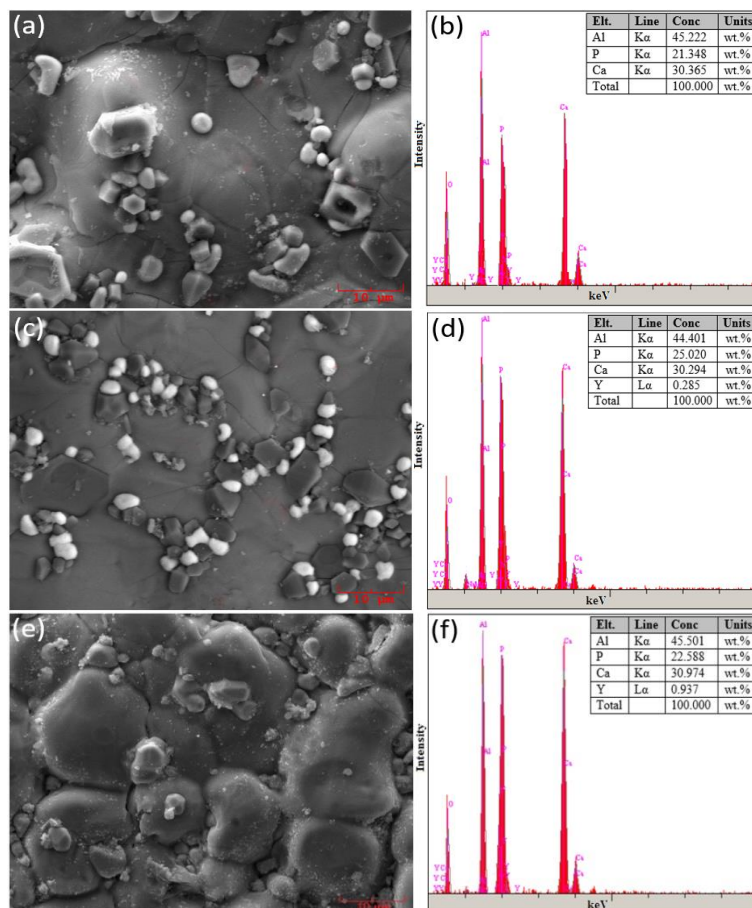


Fig. 4. SEM images and EDS spectra of the produced biocomposites after sintering at 1550°C for 4 h in air: (a) BHAA, (b) 0.5BHAA, (c) 1BHAA.

4. Conclusions

This work was studied to determine the influence of yttria of composite materials, made of hydroxyapatite, derived from bovine bone by 0.5-1 wt% Y_2O_3 addition, in order to evaluate their phase evaluation and surface morphology (grain size, shape, structure) properties. The main phases of the sintered bioceramic composites were $(CaO)(Al_2O_3)_6$, $(Ca_3(PO_4)_2)$, $Ca_9Y(PO_4)_7$ and $AlYO_3$ depending on the yttria content which are known biocompatible. The reproducible phase analyses and morphological evaluation suggest that these materials would have good performance in load bearing applications, biocompatibility issues due to high sintering characteristics and low porosity which are known as having high mechanical properties.

References

- [1] J. H. G. Rocha, A. F. Lemos, S. Agathopoulos, P. Valeiro, S. Kannan, F. N. Oktar, J. M. F. Ferreira, *Bone*, **37**, 850 (2005).
- [2] L.D. Zhou, Y.K. Liu, G.F. Zhou, *Acta Mineralogica Sinica*, **1**, 41, (1999).
- [3] X. Y. Lü, Y. B. Fan, D. Gu, W. Cui, *Key Engineering Materials*, **342-343**, 213 (2007).
- [4] G. Goller, F.N. Oktar, *Materials Letters*, **56**, 142 (2002).
- [5] Z.E. Erkmén, Y. Genc, F.N. Oktar, *Journal of the American Ceramic Society*, **90**, 2885 (2007).
- [6] A. Sobczak, Z. Kowalski, Z. Wzorek, *Acta of Bioengineering and Biomechanics*,

- 11**, 4, (2009).
- [7] O. Gunduz, S. Dağlılar, S. Salman, N. Ekren, S. Agathopoulos and F.N. Oktar, *Journal of Composite Materials*, **42**, 1281, (2008).
- [8] F.N. Oktar, S. Agathopoulos, L. S. Ozyegin, O. Gunduz, N. Demirkol, Y. Bozkurt, S. Salman, *J. Mater Sci: Mater Med*, **18**, 2137 (2007).
- [9] X. Miao, A.J. Ruys, B.K. Milthorpe, *Journal of Material Science*, **36**, 3323 (2001).
- [10] S. Özyeğin, F.N Oktar, G. Göller, E.S Kayalı, T. Yazıcı, *Materials Letters*, **58-21**, 2605 (2004).
- [11] J.H.G Rocha, A.F Lemos, S. Agathopoulos, P. Valerio, S. Kannan, F.N Oktar, J.M.F Ferreira, *Bone*, **37-6**, 850 (2005).
- [12] F.N Oktar, M. Yetmez, S. Agathopoulos, G. Lopez, G. Goller, I. Peker, J.M.F Ferreira, *Journal of Materials Science: Materials in Medicine*, **17-11**, 1161 (2006).
- [13] J. Chevalier, *Biomaterials*, **27-4**, 535 (2006).
- [14] J.J. Jerome, S. Deville, E. Munch, R. Jullian, *Biomaterials*, **25-24**, 5539, (2004).
- [15] A.B Khalil, S.W Kim, Y.K Kim, *Materials Science Engineering A* **456**, 368 (2007).
- [16] F.N Oktar, K. Kesenci, E. Pişkin, *Artificial Cell Blood Sub. Immob. Biotech*, **27**, 367 (1999).